Supplemental Materials

Molecular Biology of the Cell

Kabachinski et al.

SUPPLEMENTAL MATERIAL FOR

Resident CAPS on dense-core vesicles docks and primes vesicles for fusion

Greg Kabachinski*†, D. Michelle Kielar-Grevstad*, Xingmin Zhang, Declan J. James, Thomas F.J. Martin‡

Department of Biochemistry, University of Wisconsin, Madison WI 53706
†Department of Biology, Massachusetts Institute of Technology, Cambridge MA 02139

*G.K. and D.M. K-G. contributed equally to this work. ‡Correspondence to: T.F.J. Martin, Department of Biochemistry, 433 Babcock Drive, Madison, WI, 53706 tfmartin@wisc.edu

Defining DCV pools by mobility. For the analyses of DCV docking by TIRF microscopy, we employed the fluorescent DCV cargo BDNF-EGFP. Expression of BDNF-EGFP in PC12 cells for 48hr successfully loads the entire population of DCVs(Lynch and Martin, 2007). Adherent cells were imaged for 10s at 4Hz by TIRF microscopy with a penetration depth of 160nm to identify plasma membrane-proximal DCVs. We initially classified vesicles in the TIRF field into two pools: mobile and immobile. Mobile DCVs in the field move randomly or along actin fibers, whereas DCVs that attach to the plasma membrane exhibit strongly reduced mobility (Burke et al., 1997; Lang et al., 2000; Li et al., 2004; Nofal et al., 2007; Steyer and Almers, 1999). We eliminated the mobile pool of vesicles, as well as vesicles that transiently appeared in the field, by movement corrections to the images (see Materials and Methods), which decreased the overall DCV density within the TIRF field by 15% (Fig. S1A).

Characterization of the immobile pool. The immobile fraction of DCVs within the TIRF field (85%) contains DCVs enmeshed within the cortical actin network as well as those that directly attach to the plasma membrane. To eliminate the fraction of immobile vesicles that are actin-trapped, we treated cells with the F-actin-severing drug halichondramide (HALI). The addition of 10 μM HALI for 10 minutes reduced the amount of F-actin by 90% (not shown) and resulted in a 20% reduction of the immobile pool of DCVs (Fig. S1A). The overall results indicate that 65% of the DCVs in the TIRF field are physically attached to the plasma membrane (immobile and not actin-caged) whereas the remaining 35% are either mobile or actin-caged. Thus, single TIRF images without a mobility correction and without F-actin disassembly would considerably overestimate pools of plasma membrane-attached DCVs. Our subsequent studies of DCV attachment to the plasma membrane used these stringent criteria throughout.

Loss of t-SNAREs reduces the number of attached DCVs. We assessed roles for syntaxin-1 and SNAP-25 in vesicle attachment by depleting each t-SNARE individually or together. Morphological docking of DCVs in neuroendocrine cells was reported to be dependent on syntaxin-1 (de Wit et al., 2006; Hammarlund et al., 2008; Ohara-Imaizumi et al., 2004) whereas a dependence on SNAP-25 was controversial (de Wit et al., 2009; Sorensen et al., 2003). We found that the knockdown of syntaxin-1 resulted in a 56% decrease in plasma membrane-attached DCVs (Fig. S1B). Similarly, we observed a 43% reduction of plasma membrane-attached DCVs upon reducing SNAP-25 levels. Under our conditions, syntaxin-1 or SNAP-25

protein levels were reduced by 88% and 61%, respectively. The knockdown of both syntaxin-1 and SNAP-25 resulted in a 70% decrease in DCV density (Fig. S1B). By contrast, the depletion of the vesicle v-SNARE VAMP-2 did not affect the number of attached DCVs detected in the x-y plane (Fig. S1B) similar to results reported for chromaffin cells (de Wit et al., 2009; Toonen et al., 2006). Because complete protein knockdown was not obtained, our results indicate that minimally 70% of DCV attachments utilize t-SNARE proteins.

Supplemental Figure 1. **A.** Representative images of PC12 cell DCV density within the TIRF field before and after motion correction and after HALI treatment (scale bar 5μm). Quantitation of vesicle density before (black) and after (gray) motion correction and after HALI addition (light gray) (* $p<0.05$, *** $p<0.001$; $n\geq29$). **B.** SNARE knockdown in PC12 cells. Representative images after motion correction of HALI-treated cells (left) or cells knocked down for SNAP-25 and syntaxin-1 and HALI-treated (right). Histograms indicate quantitation of DCV densities using stringent criteria for wild-type cells (1.52±0.5, n=53) without or with HALI treatment (1.21±0.5, n=30) and HALI treatment with knockdowns for VAMP2 (1.49±0.4, n=20), SNAP-25 (0.70±0.4, n=28), syntaxin-1 (0.53±0.3, n=32), and for both SNAP-25 and syntaxin-1 (0.38±0.13, n=14) (***$p<0.001$).

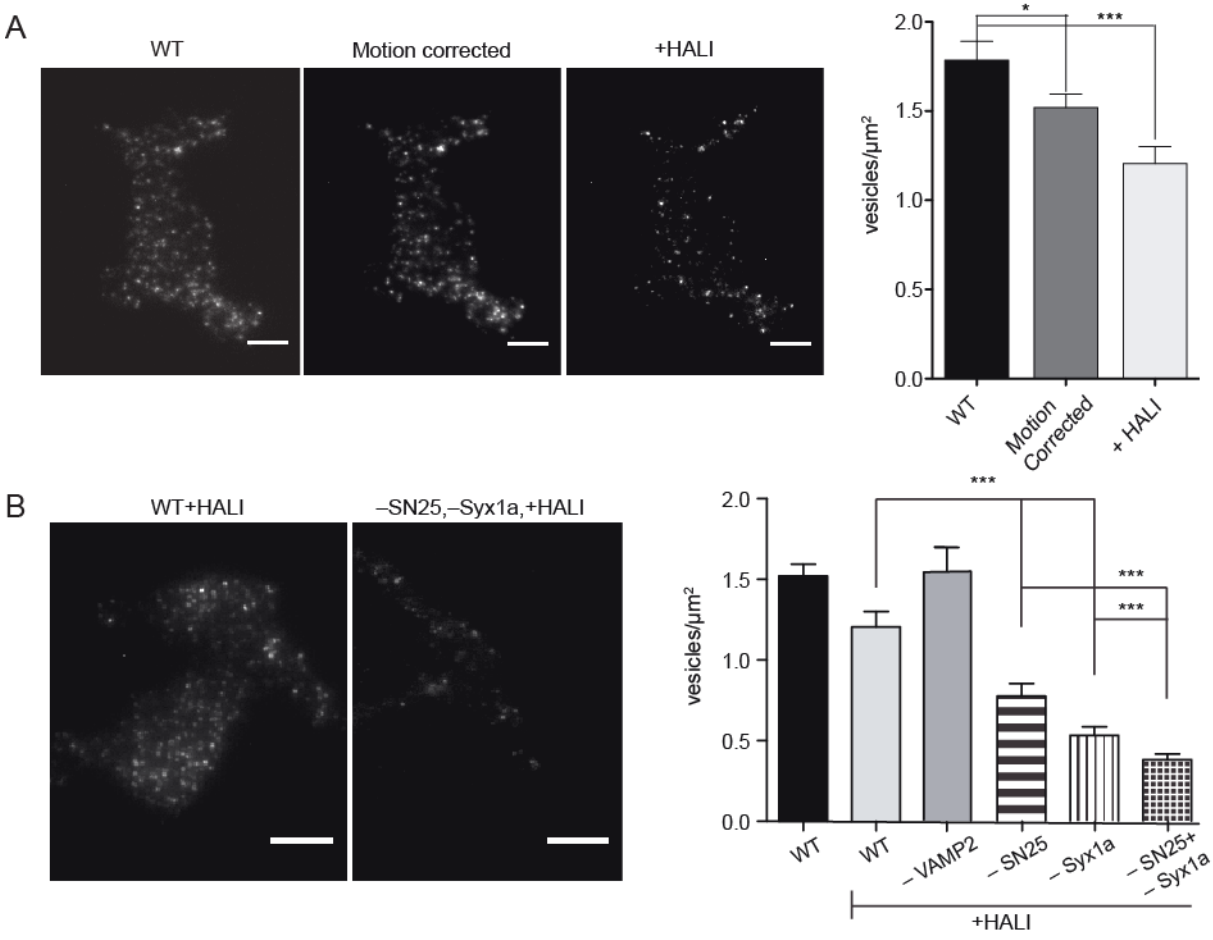

Supplemental Figure 2.**A.**DCV intensities fluctuate within the TIRF-field.Representative traces of the normalized fluorescence of individual 100nm beads, docked (pool 1), tethered(pool 2), or tethered(pool 3) vesicles within the TIRF-field over 7.5seconds. Images at 4Hz were sufficient to capture intensity changes between the peaks and valleys of individual DCVs as they move in z dimension. Differences between the minimumI_{min} and maximum intensityI_{max} were used to determine maximal movement length of an individual DCV in the TIRF-field as described in Methods. **B.** Movement of 100nm fluorescent bead within the evanescentfield. Adsorbed beads were imaged in PSS-Na +15% BSA to mimic refractive index of cell cytosol and represented in a scatter-plot of z-movement length for 2094 beads. Black bar indicates median of distribution (27nm). **C.** Movement lengths of beads were binned in 5nm increments from -2.5 to 180nm. Frequency plot was fit to a single Gaussian (least iterative fit, adjusted R-square =0.98463, Matlab).**D.**Scatter-plot of attached DCV z-movement length for wild-type (n=160 vesicles, median 29.5nm), VAMP2-deficient (n= 181, median 35.5 nm), and CAPS-deficient (n=220, median 38.7 nm), or VAMP- and CAPS-deficient PC12 cells (n=134, median 36.7 nm). Medians are indicated by black bar (ns = not significant; ** $p<0.01$).

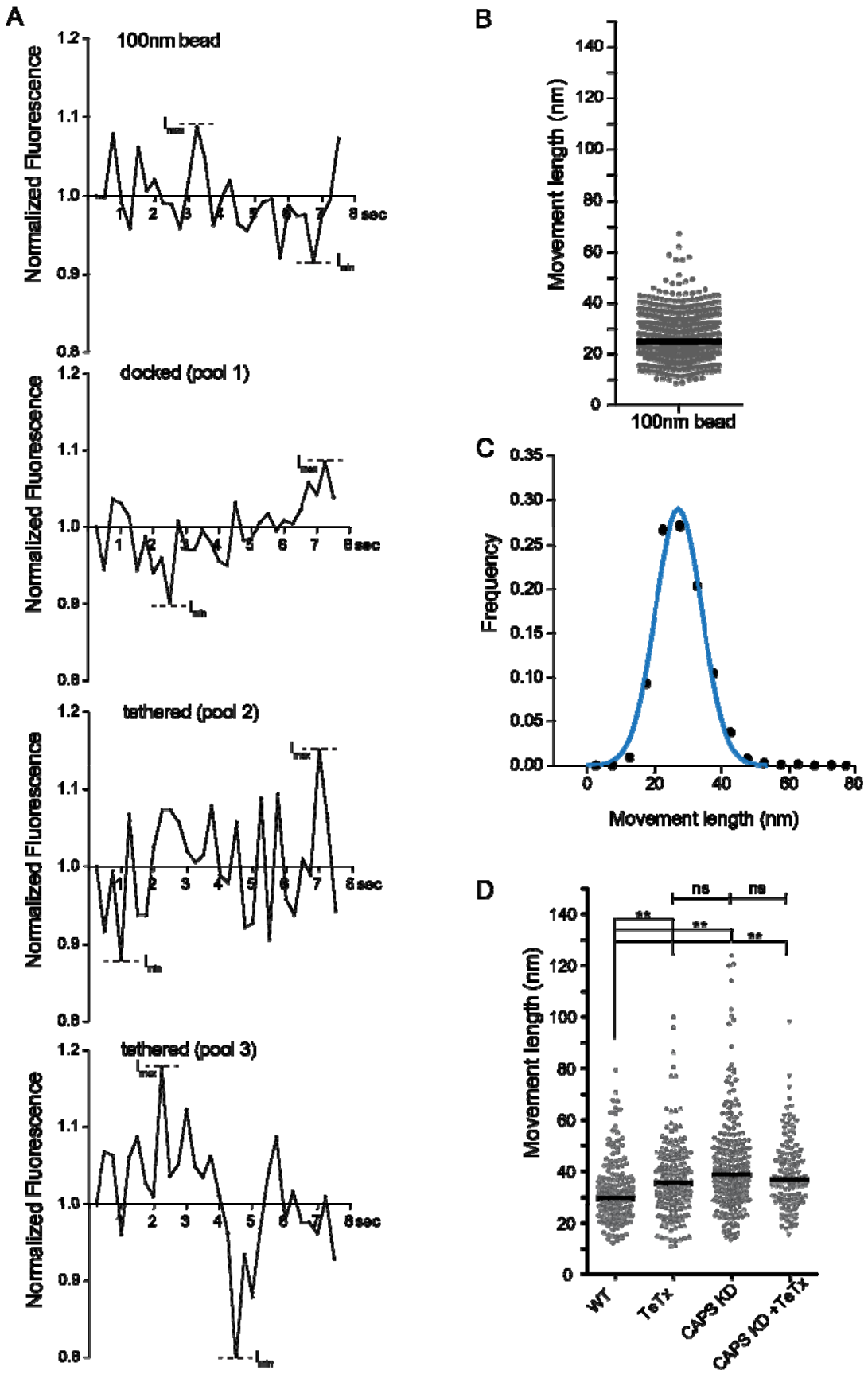
A
100nm bead
docked (pool 1)
tethered (pool 2)
tethered (pool 3)
Normalized Fluorescence
8 sec
B
Movement length (nm)
100nm bead
C
Frequency
Movement length (nm)
D
Movement length (nm)
ns
**
WT
TeTx
CAPS KD
CAPS KD +TeTx

Supplemental Movie.CAPS and DCVs move together in the TIRFfield. Video of PC12 cells expressing BDNF-eGFP (vesicle cargo) and CAPS-mKate2. Boxed region of interest highlights where a mobile DCV traverses the TIRF field (arrowheads). Images were captured at 4Hz.

References for Supplemental Information

Burke, N.V., W. Han, D. Li, K. Takimoto, S.C. Watkins, and E.S. Levitan. 1997. Neuronal peptide release is limited by secretory granule mobility. *Neuron*. 19:1095-1102.

de Wit, H., L.N. Cornelisse, R.F. Toonen, and M. Verhage. 2006. Docking of secretory vesicles is syntaxin dependent. *PLoS One*. 1:e126.

de Wit, H., A.M. Walter, I. Milosevic, A. Gulyas-Kovacs, D. Riedel, J.B. Sorensen, and M. Verhage. 2009. Synaptotagmin-1 docks secretory vesicles to syntaxin-1/SNAP-25 acceptor complexes. *Cell*. 138:935-946.

Hammarlund, M., S. Watanabe, K. Schuske, and E.M. Jorgensen. 2008. CAPS and syntaxin dock dense core vesicles to the plasma membrane in neurons. *The Journal of cell biology*. 180:483-491.

Lang, T., I. Wacker, I. Wunderlich, A. Rohrbach, G. Giese, T. Soldati, and W. Almers. 2000. Role of actin cortex in the subplasmalemmal transport of secretory granules in PC-12 cells. *Biophysical journal*. 78:2863-2877.

Li, D., J. Xiong, A. Qu, and T. Xu. 2004. Three-dimensional tracking of single secretory granules in live PC12 cells. *Biophysical journal*. 87:1991-2001.

Lynch, K.L., and T.F. Martin. 2007. Synaptotagmins I and IX function redundantly in regulated exocytosis but not endocytosis in PC12 cells. *J Cell Sci*. 120:617-627.

Nofal, S., U. Becherer, D. Hof, U. Matti, and J. Rettig. 2007. Primed vesicles can be distinguished from docked vesicles by analyzing their mobility. *The Journal of neuroscience : the official journal of the Society for Neuroscience*. 27:1386-1395.

Ohara-Imaizumi, M., C. Nishiwaki, T. Kikuta, K. Kumakura, Y. Nakamichi, and S. Nagamatsu. 2004. Site of docking and fusion of insulin secretory granules in live MIN6 beta cells analyzed by TAT-conjugated anti-syntaxin 1 antibody and total internal reflection fluorescence microscopy. *The Journal of biological chemistry*. 279:8403-8408.

Sorensen, J.B., G. Nagy, F. Varoqueaux, R.B. Nehring, N. Brose, M.C. Wilson, and E. Neher. 2003. Differential control of the releasable vesicle pools by SNAP-25 splice variants and SNAP-23. *Cell*. 114:75-86.

Steyer, J.A., and W. Almers. 1999. Tracking single secretory granules in live chromaffin cells by evanescent-field fluorescence microscopy. *Biophysical journal*. 76:2262-2271.

Toonen, R.F., O. Kochubey, H. de Wit, A. Gulyas-Kovacs, B. Konijnenburg, J.B. Sorensen, J. Klingauf, and M. Verhage. 2006. Dissecting docking and tethering of secretory vesicles at the target membrane. *The EMBO journal*. 25:3725-3737.